LA-UR-06-3853

Approved for public release; distribution is unlimited.

Title: Shock Wave Solutions for Equilibrium-Diffusion Radiation Hydrodynamics

Author(s): R. B. Lowrie (CCS-2)
R. M. Rauenzahn (T-3)

Submitted to: General Distribution

Los Alamos NATIONAL LABORATORY

research note

Weapons Supported Research

Radiation Hydrodynamics

To/MS: Distribution
From/MS: Robert B. Lowrie/CCS-2, MS D413
Rick M. Rauenzahn/T-3, MS B216
Phone/FAX: (505)667–2121

Symbol: LA-UR-06-3853
Date: May 31, 2006

Subject: Shock Wave Solutions for Equilibrium-Diffusion Radiation Hydrodynamics

Revision: 1

Executive Summary

A semi-analytic solution is described for planar radiation-hydrodynamic shock waves in the equilibrium-diffusion (1-T) limit. The solution requires finding numerically the root of a polynomial and integrating a nonlinear ordinary differential equation. This solution may be used to verify codes that use the equilibrium-diffusion radiation model, or for more advanced radiation models in the optically-thick limit. The conditions for continuous solutions are also discussed.

1 Introduction

This study details a semi-analytic solution for planar radiation-hydrodynamic shock waves in the equilibrium-diffusion (1-T) limit. The solution may be used to verify codes that use the equilibrium-diffusion radiation model. Moreover, any radiation model should be able to compute these shocks when in the optically-thick limit.

Radiation-hydrodynamic shocks are described in detail by Zel'dovich and Raizer [1] and Mihalas and Mihalas [2]. However, the solutions in past work are typically approximate and thus inappropriate for code verification. The focus of this study is to:

1. review the past work on radiation-hydrodynamic shocks,
2. derive the equations for the semi-analytic solution,
3. present the numerical solution procedure and example solutions,
4. discuss the regimes where the solution is continuous.

The shock structure for nonequilibrium radiation models is more complicated than for the equilibrium-diffusion model and these differences will also be highlighted.

2 Equilibrium-Diffusion System

Assume a single material, strength or viscous effects are negligible, the radiation optical depth is small, and material speeds are non-relativistic. Then radiation hydrodynamics is described by the equilibrium-diffusion system, which may be written in nondimensional form as (see, for example, [2, 3])

$$\partial_t \begin{pmatrix} \rho \\ \rho v \\ \rho E^* \end{pmatrix} + \partial_x \begin{pmatrix} \rho v \\ \rho v^2 + p^* \\ (\rho E^* + p^*)v \end{pmatrix} = \partial_x \begin{pmatrix} 0 \\ 0 \\ \kappa \partial_x T^4 \end{pmatrix}, \tag{1a}$$

where

$$p^* = p + \frac{1}{3}\mathcal{P}T^4, \tag{1b}$$

$$e^* = e + \frac{1}{\rho}\mathcal{P}T^4, \tag{1c}$$

$$E^* = e^* + \frac{1}{2}v^2, \tag{1d}$$

and $\mathcal{P}$ is a nondimensional constant. The material's equation-of-state (EOS) is assumed to be of the form $p(\rho, T)$ and $e(\rho, T)$. For this radiation model, the radiation effectively modifies the material EOS to $p^*(\rho, T)$ and $e^*(\rho, T)$. See Ref. [3] for an analysis of the radiation-modified EOS.

In this study, dimensional quantities are denoted with a tilde; for example, $\tilde{p}$. The nondimensional variables are defined in terms of their dimensional counterparts as

$$x = \frac{\tilde{x}}{\tilde{L}}, \quad t = \frac{\tilde{t}\tilde{a}_0}{\tilde{L}}, \quad \rho = \frac{\tilde{\rho}}{\tilde{\rho}_0}, \quad v = \frac{\tilde{v}}{\tilde{a}_0}, \tag{2}$$
$$e = \frac{\tilde{e}}{\tilde{a}_0^2}, \quad p = \frac{\tilde{p}}{\tilde{\rho}_0\tilde{a}_0^2}, \quad T = \frac{\tilde{T}}{\tilde{T}_0}, \quad \kappa = \frac{\tilde{\kappa}\tilde{T}_0^4}{\tilde{\rho}_0\tilde{a}_0^3\tilde{L}},$$

where the subscript-"$_0$" indicates a constant reference state. Here $\tilde{a}$ refers to the material soundspeed and $\tilde{L}$ is a reference length. The dimensional diffusion coefficient may be written as

$$\tilde{\kappa} = \frac{\tilde{\alpha}_R\tilde{c}}{3\tilde{\sigma}_t}, \tag{3}$$

where $\tilde{\alpha}_R$ is the radiation constant ($7.55 \times 10^{-16} N/(K^4 m^2)$), $\tilde{c}$ the speed of light ($3 \times 10^8 m/s$), and σ_t the total radiation cross-section. The nondimensional constant $\mathcal{P}$ is given by

$$\mathcal{P} = \frac{\tilde{\alpha}_R\tilde{T}_0^4}{\tilde{\rho}_0\tilde{a}_0^2}. \tag{4}$$

For a given EOS, the character of the solution is determined by the shock Mach number ($\mathcal{M}$), the κ function, and $\mathcal{P}$. The function κ controls the amount of thermal diffusion and in particular, the extent of the radiation precursor in front of the shock. The constant $\mathcal{P}$ is a measure of the influence of radiation on the flow dynamics; $\mathcal{P}$ is proportional to the ratio of radiation pressure to material pressure or alternatively, radiation energy to material energy. The "low-energy density" regime assumes that the $\mathcal{P}T^4$ terms are small in Eqs. (1b,1c), so that $e^* \to e$ and $p^* \to p$. The "high-energy density" regime retains these terms and is the focus of this study.

3 Problem Statement

We will select a reference frame where the shock speed is zero. The non-zero shock speed case may be found through a Galilean transformation. The reference state (subscript-$_0$) will refer to the far upstream conditions ($x \to -\infty$), while the subscript-$_1$ refers to far downstream conditions ($x \to \infty$), with $v_0 \equiv \mathcal{M} > 1$. Note that in the shock reference frame, $\mathcal{M}$ is the upstream Mach number with respect to the material soundspeed. Also, the normalization (2) gives that $\rho_0 = 1 = T_0$.

The problem statement is then as follows:

- *Given:*
  - The values $\mathcal{P}$ and $\mathcal{M}$.
  - The functions $p(\rho, T)$, $e(\rho, T)$, $\kappa(\rho, T)$.

- *Calculate:*
  - The functions $\rho(x)$, $v(x)$, $T(x)$.

Much of the previous work on this problem is described in Zel'dovich and Raizer [1] and Mihalas and Mihalas [2]. The shock problem is a specific case of the class of equilibrium-diffusion, radiation-hydrodynamic solutions derived by Coggeshall and Axford [4]. Recent work on the shock problem is also given in Ref. [5]. For the low-energy density regime, see also the classic blast-wave solution in Ref. [6]. Non-equilibrium shock solutions are described in Refs. [1, 2, 7–10].

4 Solution Phenomenology

In this section, we review the structure of radiation-hydrodynamic shock waves. The physics of these shocks is explained very well in Refs. [1, 2, 7–9]; only the minimum information needed will be repeated here.

First, we'll describe the shock structure for a non-equilibrium model of radiation, following Refs. [1,2,8,9]. As the material moves through the shock structure, it passes through several regions, in the following order:

1. *Radiation Precursor:* The hot post-shock material radiates, heating the flow ahead of the shock from $T = T_0$ to $T = T_p > T_0$. The value of T_p determines the character of the shock:
   - Subcritical shock: $T_p < T_1$.
   - Supercritical shock: $T_p \equiv T_1$.

   See Fig. 1.
2. For supercritical shocks and if $\rho_p \equiv \rho_1$, then all variables are continuous through the shock profile. If instead $\rho_p < \rho_1$ (true for all subcritical shocks), then the flow passes next through the following regions:
   (a) *Hydrodynamic Shock:* A hydrodynamic shock then further heats the material from $T = T_p$ to $T = T_s > T_1$. For the Euler equations, this heating is discontinuous. Note that even if the the state-$_p$ conditions are in radiative equilibrium, the hydrodynamic shock discontinuity breaks equilibrium; the state-$_s$ is always a non-equilibrium state. The spike to $T = T_s$ is referred to as the *Zel'dovich spike* [2, 8, 9].
   (b) *Relaxation Region:* Through radiative cooling, the material cools from $T = T_s$ to its final post-shock state, $T = T_1$. The width of the relaxation region is proportional to the post-shock optical depth.

The equilibrium-diffusion shock structure is simpler than the general picture. Mathematically, because of the diffusion term in the system (1), the temperature for this model *must* be continuous. Consequently, the nearest temperature profile that may be represented by the equilibrium-diffusion model is the supercritical profile, but that ignores the Zel'dovich spike and its subsequent relaxation region. Roughly speaking, because the optical depth must be small for the equilibrium-diffusion system (1) to apply, and the spike width is proportional to the optical depth, it seems reasonable to ignore the spike region.

The equilibrium-diffusion shock structure is then as follows (see Fig. 1b):

1. *Radiation Precursor:* Same as non-equilibrium model, supercritical shock case. If $\rho_p \equiv \rho_1$, then all variables are continuous through the shock profile. If instead $\rho_p < \rho_1$, then the flow passes through an isothermal shock.
2. *Isothermal Shock:* An isothermal, hydrodynamic shock transitions the flow from $(\rho, v)_p$ to $(\rho, v)_1$. We emphasize that $T_p = T_1$. There is no relaxation region after the shock.

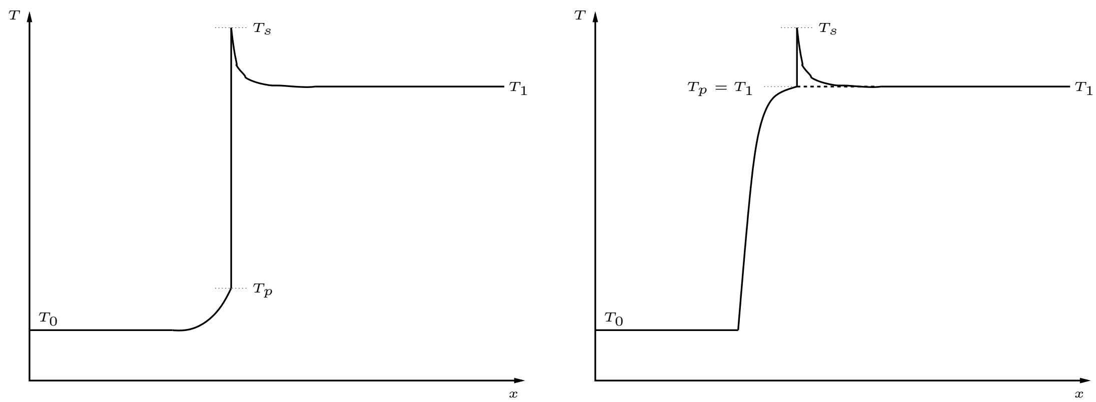

(a) Subcritical (b) Supercritical

Figure 1: Subcritical and supercritical ($\rho_p < \rho_1$) shock structures. Only non-equilibrium radiation models will produce the subcritical solution. In both cases, the temperature is discontinuous from T_p to T_s. In the supercritical case, non-equilibrium models can compute the Zel'dovich spike ($T = T_s$) region, whereas the equilibrium-diffusion structure follows the dashed line.

Although the equilibrium-diffusion model ignores the Zel'dovich spike, one can nevertheless estimate the spike's maximum temperature. We will discuss the Zel'dovich spike further in §7.

The solution procedure is then as follows:

1. *Determine the Overall Shock Jump:* Apply the overall Rankine-Hugoniot jump relations, including radiation effects, to determine the far downstream state $(\rho, v, T)_1$.

2. *Determine the Radiation Precursor:* The radiation precursor is found by integrating the diffusion operator from temperature $T = T_p (= T_1)$ to $T = T_0$.

3. *Determine the Zel'dovich Spike:* This step is optional and applies only if $\rho_p < \rho_1$. Knowing the conditions at the precursor state, $(\rho, v, T)_p$, one is only able to compute the spike conditions $(\rho, v, T)_s$. The temperature profile of the relaxation region requires a non-equilibrium model.

Each of these steps is described in the following sections.

5 Overall Shock Jump

This section is actually applicable to any radiation model, if it is assumed that the radiation and hydrodynamics equilibrate far from the shock. In a reference frame where the shock speed is zero, the jump conditions for Eq. (1) are

$$\begin{pmatrix} \rho v \\ \rho v^2 + p^* \\ (\rho E^* + p^*) v \end{pmatrix}_0 = \begin{pmatrix} \rho v \\ \rho v^2 + p^* \\ (\rho E^* + p^*) v \end{pmatrix}_1 \tag{5}$$

Note that the radiation terms are proportional to $\mathcal{P}$ and are independent of κ. The velocities may be eliminated to yield the Hugoniot relation

$$e_1^* - e_0^* + \frac{1}{2}(p_0^* + p_1^*) \left(\frac{1}{\rho_1} - \frac{1}{\rho_0} \right) = 0. \tag{6}$$

Also, v_1 may be eliminated from the mass and momentum equations to give

$$\frac{p_1^* - p_0^*}{\rho_1 - \rho_0} = \mathcal{M}^2 \frac{\rho_0}{\rho_1}. \tag{7}$$

If $\mathcal{P}$ and the upstream ("$_0$") conditions are given, then Eqs. (6) and (7) are two equations for two unknowns, ρ_1 and T_1. Mass conservation may then be used to find v_1:

$$v_1 = \frac{\rho_0 \mathcal{M}}{\rho_1}. \tag{8}$$

Just as for the pure hydro case ($\mathcal{P} \equiv 0$), an entropy condition must be invoked to ensure uniqueness. The entropy s^* follows from the concept of a radiation-modified EOS [3] and satisfies

$$T ds^* = de^* + p^* d\left(\frac{1}{\rho}\right). \tag{9}$$

The entropy condition for the shock is $s_1^* \geq s_0^*$, which requires

$$\mathcal{M} \geq a_0^*, \tag{10}$$

where a^* is the radiation-modified soundspeed. See Ref. [3] for the expression for a^* for a general EOS.

5.1 Shock Jump for a γ-Law EOS

A γ-law EOS assumption simplifies matters somewhat. In this case, $\tilde{a}_0^2 = \gamma R \tilde{T}_0$ and $\tilde{p} = \tilde{\rho} R T$, where R is the material gas constant and γ the ratio of specific heats. In nondimensional form, the EOS becomes

$$p(\rho, T) = \frac{\rho T}{\gamma}, \qquad e(\rho, T) \equiv e(T) = \frac{T}{\gamma(\gamma - 1)}. \tag{11}$$

In order to shorten the expressions, this section will use the fact that $\rho_0 = 1 = T_0$. The radiation-modified soundspeed in (10) may be written as [3]

$$(a_0^*)^2 = 1 + \frac{4}{9}\mathcal{P}(\gamma - 1)\frac{4\mathcal{P}\gamma + 3(5 - 3\gamma)}{1 + 4\mathcal{P}\gamma(\gamma - 1)}. \tag{12}$$

Equation (6) is a quadratic in ρ_1 and the positive root is

$$\rho_1(T_1) = \frac{b(T_1) + \sqrt{b(T_1)^2 + 12(\gamma - 1)^2 T_1 \left[3 + \gamma\mathcal{P}(1 + 7T_1^4)\right]}}{6(\gamma - 1)T_1}, \tag{13}$$

where

$$b(T_1) = 3(\gamma + 1)(T_1 - 1) - \mathcal{P}\gamma(\gamma - 1)(7 + T_1^4). \tag{14}$$

Equation (7) may be written as

$$3\rho_1(\rho_1 T_1 - 1) + \gamma\mathcal{P}\rho_1(T_1^4 - 1) = 3\gamma(\rho_1 - 1)\mathcal{M}^2. \tag{15}$$

Combined with Eq. (13), the expression (15) represents a single equation for the unknown T_1. Although we prefer the form of Eqs. (13,15), they may also be manipulated into a single ninth-order polynomial for T_1 [5].

In general, no closed-form solution for T_1 exists; Eq. (15) must be solved numerically. For small $\mathcal{P}$, a reasonable initial guess is the $\mathcal{P} = 0$ solution:

$$T_1 = \frac{(1 - \gamma + 2\gamma\mathcal{M}^2)(2 + (\gamma - 1)\mathcal{M}^2)}{(\gamma + 1)^2\mathcal{M}^2}. \tag{16}$$

In the limit of large $\mathcal{P}$, Eq. (13) reduces to

$$\rho_1(T_1) \approx \frac{1+7T_1^4}{7+T_1^4}. \tag{17}$$

Note that the maximum compression is given by $\rho_1 = 7$ and corresponds to the maximum for $\gamma = 4/3$, which is the effective γ for photons. Also, Eq. (12) becomes

$$(a_0^*)^2 \approx \frac{4}{9}\mathcal{P} \tag{18}$$

for large $\mathcal{P}$. The effective Mach number may be defined as

$$\mathcal{M}^* = \mathcal{M}/a_0^*. \tag{19}$$

It follows that Eq. (15) reduces to

$$\gamma\mathcal{P}\rho_1(T_1^4 - 1) \approx 3\gamma(\rho_1 - 1)(\mathcal{M}^*)^2\left(\frac{4}{9}\mathcal{P}\right). \tag{20}$$

Using Eq. (17), this relation reduces to

$$T_1^4 \approx \frac{1}{7}[8(\mathcal{M}^*)^2 - 1]. \tag{21}$$

6 Radiation Precursor

Knowing the overall shock jump from the previous section, the radiation precursor may now be determined. Integrate once the steady-state energy equation of the system (1) to obtain

$$4\kappa T^3\frac{dT}{dx} = \left(\rho e + p + \frac{1}{2}\rho v^2 + \frac{4}{3}\mathcal{P}T^4\right)v - \left(e_0 + p_0 + \frac{1}{2}\mathcal{M}^2 + \frac{4}{3}\mathcal{P}\right)\mathcal{M}, \tag{22}$$

where the integration constant was evaluated so that the derivative vanishes at the reference state ("$_0$"). Mass conservation gives

$$v = \mathcal{M}/\rho, \tag{23}$$

so that Eq. (22) may be written as

$$4\kappa T^3\frac{dT}{dx} = \mathcal{M}\left[e - e_0 + \frac{p}{\rho} - p_0 + \frac{1}{2}\mathcal{M}^2\left(\frac{1}{\rho} - 1\right) + \frac{4}{3}\mathcal{P}\left(\frac{T^4}{\rho} - 1\right)\right]. \tag{24}$$

Momentum conservation gives

$$p - p_0 = \mathcal{M}^2\left(1 - \frac{1}{\rho}\right) + \frac{1}{3}\mathcal{P}\left(1 - T^4\right). \tag{25}$$

Given $e(\rho, T)$ and $p(\rho, T)$, in general Eqs. (24,25) must be integrated numerically in order to find the shock profile.

6.1 Precursor for a γ-Law EOS

For a γ-law EOS, Eq. (24) becomes

$$\frac{dT}{dx} = \frac{6C_p(T-1)\rho^2\mathcal{M} + 3(1-\rho^2)\mathcal{M}^3 + 8\mathcal{P}(T^4 - \rho)\rho\mathcal{M}}{24\kappa\rho^2T^3}, \tag{26}$$

where

$$C_p = \frac{1}{\gamma - 1}. \tag{27}$$

Equation (25) becomes a quadratic in $\rho(T)$ whose solution is

$$\rho(T) = \frac{m(T) - \sqrt{m(T)^2 - \gamma T \mathcal{M}^2}}{T}, \tag{28}$$

where

$$m(T) = \frac{1}{2}(\gamma \mathcal{M}^2 + 1) + \frac{\gamma \mathcal{P}}{6}(1 - T^4). \tag{29}$$

Here, the root was chosen that satisfies $\rho(T_0) = \rho_0 = 1$.

The right-hand-side of Eq. (26) may now be expressed solely as a function of T and may be integrated numerically. The integration begins at $T = T_1$, where we arbitrarily set $x = 0$. The temperature profile is computed by integrating (26) to $x \to -\infty$, or until the right-hand side of (26) is sufficiently small.

We also now have enough information to compute the precursor state $(\rho, v, T)_p$. Equation (28), evaluated at $T = T_p = T_1$, gives ρ_p. Then, Eq. (23) may be used to compute v_p.

7 Isothermal Shock and the Zel'dovich Spike

If the $\rho_p < \rho_1$, then an isothermal shock jump is present in the equilibrium-diffusion solution. The isothermal shock transitions the state $(\rho, v, T)_p$ to $(\rho, v, T)_1$, with $T_1 = T_p$. For nonequilibrium radiation models, the condition $\rho_p < \rho_1$ will create a Zel'dovich spike. Although solutions to the equilibrium-diffusion equations do not predict the Zel'dovich spike, the spike state $(\rho, v, T)_s$ may nevertheless be estimated from an equilibrium-diffusion solution. This is because for supercritical shocks, the precursor and spike states are solely a function of the overall jump conditions, and thus are independent of radiation model employed. With additional simplifying assumptions than made here, other estimates for T_s are given in Refs. [1, 2].

The assumption made here is that the hydrodynamic deviations from a Maxwellian velocity distribution (*e.g.*, viscous effects) occur on a much smaller length scale than radiation effects. In other words, the Euler equations hold, even on what may be very small length scales. Consequently, the jump from the state $(\rho, v, T)_p$ to $(\rho, v, T)_s$ is governed by a hydrodynamic shock. For a γ-law EOS, the spike values may be found by using the classic hydro-only shock relations:

$$\rho_s = \rho_p \frac{(\gamma + 1)\mathcal{M}_p^2}{2 + (\gamma - 1)\mathcal{M}_p^2}, \tag{30a}$$

$$v_s = \mathcal{M}/\rho_s, \tag{30b}$$

$$T_s = T_p \frac{(1 - \gamma + 2\gamma \mathcal{M}_p^2)(2 + (\gamma - 1)\mathcal{M}_p^2)}{(\gamma + 1)^2 \mathcal{M}_p^2}, \tag{30c}$$

where $\mathcal{M}_p$ is the Mach number at state-$_p$:

$$\mathcal{M}_p = \frac{v_p}{\sqrt{T_p}}. \tag{30d}$$

Again, to compute the temperature relaxation region downstream of T_s requires a non-equilibrium radiation model; see [7–10].

7.1 Conditions for an Isothermal Shock

As discussed above, if $\rho_p < \rho_1$, an isothermal shock exists in the equilibrium-diffusion solution and a Zel'dovich spike in nonequilibrium radiation models. In this section, we discuss the ranges of $\mathcal{M}$ and $\mathcal{P}$ that give $\rho_p < \rho_1$. Following [1, Ch. VII, §18], the $\rho_p < \rho_1$ condition can also be stated as $\eta_1 < \eta_{\max}$, where $\eta = 1/\rho$ and $\eta_{\max}$ is to be determined.[1]

The value of $\eta_{\max}$ may be determined as follows. For any point on the Hugoniot, Eq. (15) may be written as

$$T - \eta + \alpha\eta(T^4 - 1) = \gamma\eta(1-\eta)\mathcal{M}^2, \tag{31}$$

where $\alpha = \gamma\mathcal{P}/3$. This is a relation for $\eta(T)$, which has a maximum at

$$\eta_{\max} = \frac{1}{2} - \frac{1}{2\gamma\mathcal{M}^2}\left[\alpha T_{\max}^4 - \alpha - 1\right]. \tag{32}$$

Solve (32) for $T_{\max}$ and substitute back into Eq. (31) for T to obtain

$$\alpha(\gamma\eta_{\max}^2\mathcal{M}^2)^4 = 1 + \alpha + (1 - 2\eta_{\max})\gamma\mathcal{M}^2. \tag{33}$$

The relation (33) may be used to determine the boundary between solutions that contain an isothermal shock, and those that are continuous in all variables. The boundary is whenever $\eta_{\max} = \eta_1$, which may be determined numerically and is plotted in Fig. 2 for $\gamma = 5/3$.

If $\mathcal{P}$ is large enough, then an isothermal shock does not appear for any $\mathcal{M}$. For $\gamma = 5/3$ we maximized numerically $\mathcal{P}(\mathcal{M})$ in equation (33) to give $\mathcal{P} \gtrapprox 2.53$ as the condition for continuous solutions (see Fig. 2). Note also that Eq. (17) was derived for large $\mathcal{P}$ and holds anywhere along the profile; Eq. (17) also implies that ρ is continuous.

For small values of $\mathcal{P}$, it's apparent that an isothermal shock will occur over a range of $\mathcal{M}$; following Ref. [5], we denote this range as

$$\mathcal{M}_{\rm iso} < \mathcal{M} < \mathcal{M}_{\rm cont}. \tag{34}$$

We can estimate $\mathcal{M}_{\rm iso}$ and $\mathcal{M}_{\rm cont}$ as follows. The value of $\mathcal{M}_{\rm iso}$ is determined by ignoring the radiation terms in Eq. (33) (set $\alpha = 0$) and using the hydro-only shock value for η_1; see [1, Ch. VII, §3]. We obtain

$$\mathcal{M}_{\rm iso} \approx \sqrt{\frac{3\gamma - 1}{\gamma(3-\gamma)}}. \tag{35}$$

An estimate for $\mathcal{M}_{\rm cont}$ is a bit more difficult. By ignoring the upstream material temperature and pressure, Zel'dovich and Raizer derived the following estimate for $\eta_{\max}$ [1, Eq. (7.76)]:

$$\eta_{\max,\rm ZR} = \frac{1}{4 + \sqrt{2 + \rho_{10}}}, \tag{36}$$

where $\rho_{10} = (\gamma+1)/(\gamma-1)$. We expect $\mathcal{M}_{\rm cont}$ to be large, so terms that are not proportional to $\mathcal{M}$ may be dropped from Eq. (33). Solve the resulting expression for $\mathcal{M}$ and evaluate at $\eta_{\max} = \eta_{\max,\rm ZR}$ to obtain:

$$\mathcal{M}_{\rm cont} \approx \left(\frac{1 - 2\eta_{\max,\rm ZR}}{\alpha\gamma^3\eta_{\max,\rm ZR}^8}\right)^{1/6}. \tag{37}$$

The estimates $\mathcal{M}_{\rm iso}$ and $\mathcal{M}_{\rm cont}$ are shown in Fig. 2. These estimates are very accurate for small $\mathcal{P}$.

Also shown in Fig. 2 is an alternative estimate for $\mathcal{M}_{\rm cont}$, given in Bouquet et al [5]:

$$\mathcal{M}_{\rm cont}(\text{Bouquet el al}) = \left(\frac{5(7^7)}{6\alpha\gamma^3}\right)^{1/6}, \tag{38}$$

which has the correct trend, but is not as accurate for small $\mathcal{P}$ as Eq. (37).

[1] Reference [5] states incorrectly that the condition for no isothermal shock, for large $\mathcal{M}$, as $\eta_{\max} \le 1/7$.

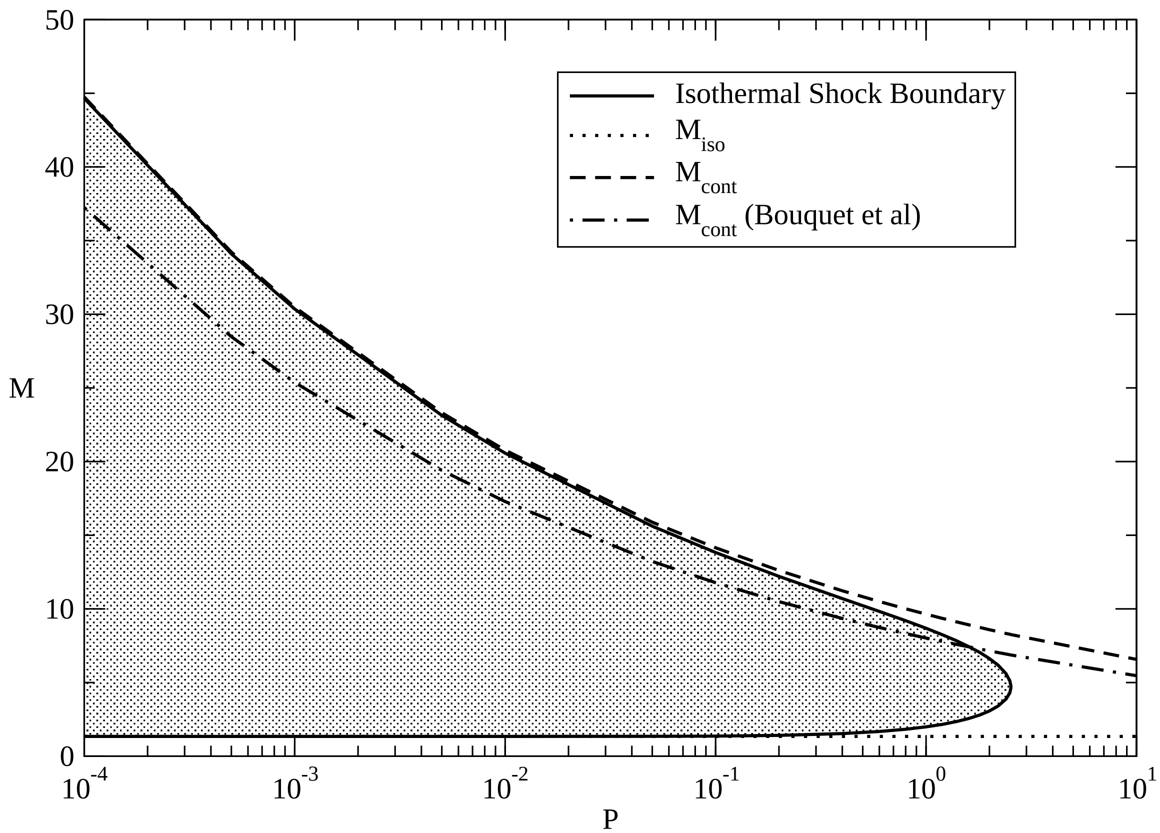

Figure 2: The isothermal shock region for $\gamma = 5/3$. The shaded region indicates $\mathcal{P}, \mathcal{M}$ pairs that result in an isothermal shock. No isothermal shock exists if $\mathcal{P} \gtrapprox 2.53$, for any $\mathcal{M}$. The estimate $\mathcal{M}_{\rm iso}$ is given by Eq. (34), $\mathcal{M}_{\rm cont}$ by Eq. (37), and "$\mathcal{M}_{\rm cont}$ (Bouquet et al)" by Eq. (38).

8 Summary

For a γ-law EOS, the calculation of the shock solution may be summarized as follows:

1. Given: $\mathcal{P}$, $\mathcal{M}$, γ, $\kappa(\rho, T)$. Recall that we use nondimensional variables so that $\rho_0 = 1 = T_0$. Also, $\mathcal{M}$ must satisfy the inequality (10).
2. Using Eq. (13) for $\rho_1(T)$, solve Eq. (15) for T_1.
3. Knowing T_1, Eq. (13) gives ρ_1.
4. Use Eq. (8) to compute v_1.
5. Use Eq. (28) to integrate (26) from $x = 0$ (where $T = T_p = T_1$), in the $(-x)$-direction. This gives $T(x)$ in the precursor region.
6. Knowing $T(x)$, compute $\rho(x)$ and $v(x)$, using Eqs. (28,23).
7. Optional: For cases where $\rho_p < \rho_1$, an isothermal shock exists. Estimate the Zel'dovich spike state using Eqs. (30).
8. Optional: Apply a Galilean transformation to a reference frame where the shock is moving with velocity v_s. Specifically, set $v := v + v_s$.

Sample calculations are given in Figs. 3-6. In Figs. 3-5, the Mach number is varied through the isothermal shock and continuous regimes. Figure 6 shows the effect of using a nonlinear diffusion coefficient, with a bremsstrahlung-like functional dependence [1].

These calculations were for a γ-law gas and future work should consider a more general EOS. The main difficulty with a general EOS is that Eq. (25) is then an implicit function for $\rho(T)$, which must be solved numerically in each integration step of Eq. (24). The overall jump conditions are also more complicated and solutions for a general EOS have been covered extensively in the literature.

References

[1] Y. B. Zel'dovich and Y. P. Raizer, *Physics of Shock Waves and High-Temperature Hydrodynamic Phenomena*. Dover, 2002.

[2] D. Mihalas and B. W. Mihalas, *Foundations of Radiation Hydrodynamics*. Oxford University Press, New York, 1984.

[3] R. Lowrie and J. Morel, "Issues with high-resolution Godunov methods for radiation hydrodynamics," *Journal of Quantitative Spectroscopy & Radiative Transfer*, vol. 69, no. 4, pp. 475–489, 2001.

[4] S. V. Coggeshall and R. A. Axford, "Lie group invariance properties of radiation hydrodynamics equations and their associated similarity solutions.," *Physics of Fluids*, vol. 29, no. 8, pp. 2398 – 420, 1986.

[5] S. Bouquet, R. Teyssier, and J. P. Chieze, "Analytical study and structure of a stationary radiative shock.," *Astrophysical Journal Supplement Series*, vol. 127, no. 2, pp. 245 – 52, 2000.

[6] P. Reinicke and J. Meyertervehn, "The point explosion with heat conduction.," *Physics of Fluids A (Fluid Dynamics)*, vol. 3, no. 7, pp. 1807 – 18, 1991.

[7] M. A. Heaslet and B. S. Baldwin, "Predictions of structure of radiation-resisted shock waves," *Physics of Fluids*, vol. 6, no. 6, pp. 781 – 791, 1963.

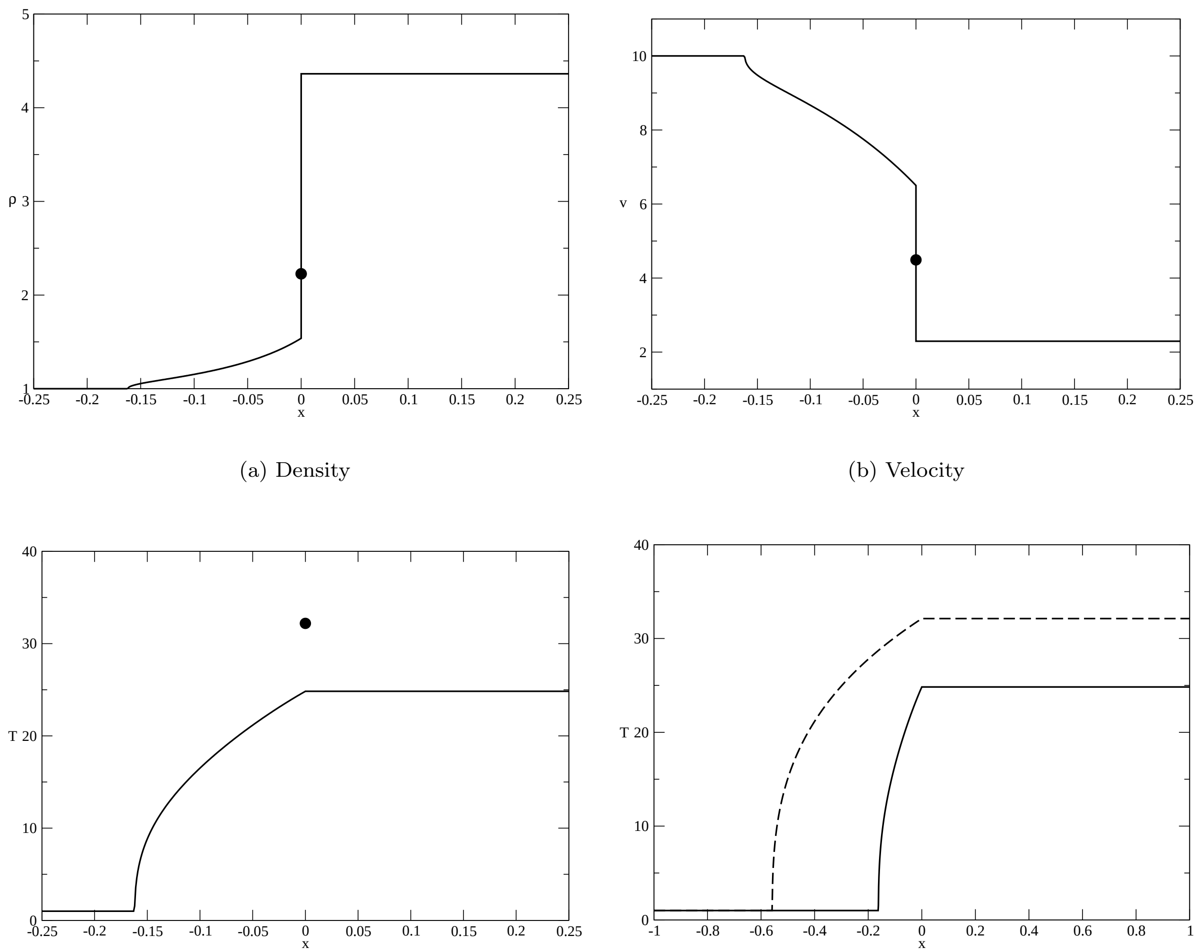

(a) Density (b) Velocity

(c) Temperature (d) Temperature. Dashed line is $\mathcal{P} = 0$ solution.

Figure 3: Shock profile for $\gamma = 5/3$, $\mathcal{M} = 10$, $\kappa = 0.0001$, $\mathcal{P} = 0.0001$. For this case, $\mathcal{M}_{\rm iso} < \mathcal{M} < \mathcal{M}_{\rm cont}$, so an isothermal shock exists. The symbol in plots (a), (b), and (c) indicates the Zel'dovich spike value. Plot (d) compares T with the low-energy density ($\mathcal{P} = 0$) solution.

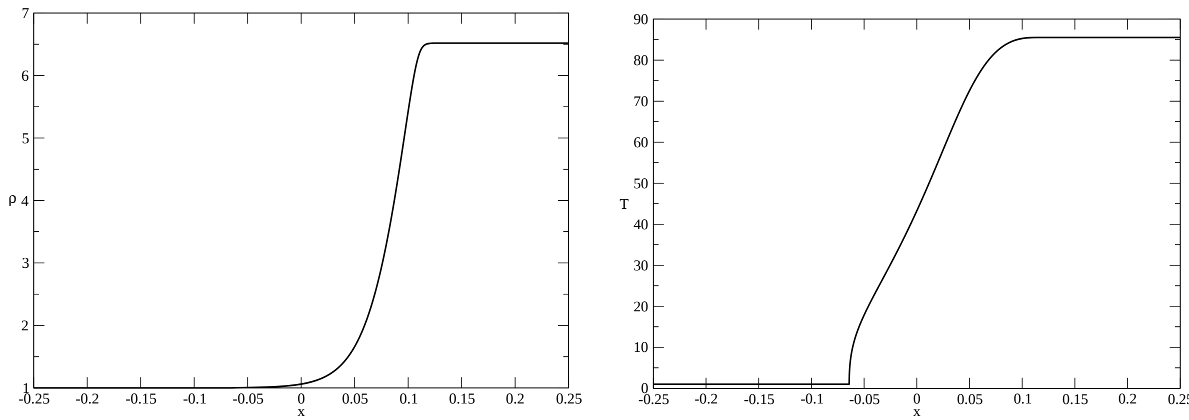

(a) Density (b) Temperature

Figure 4: Same parameters as Fig. 3, but with $\mathcal{M} = 50$. For this case, $\mathcal{M} > \mathcal{M}_{\text{cont}}$, so that all variables are continuous through the profile.

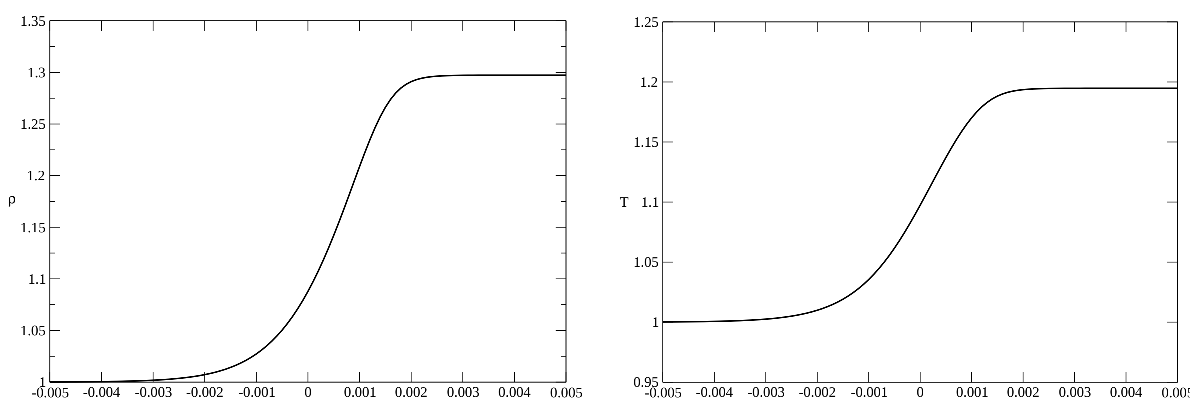

(a) Density (b) Temperature

Figure 5: Same parameters as Fig. 3, but with $\mathcal{M} = 1.2$. For this case, $\mathcal{M} < \mathcal{M}_{\text{iso}}$, so that all variables are continuous through the profile.

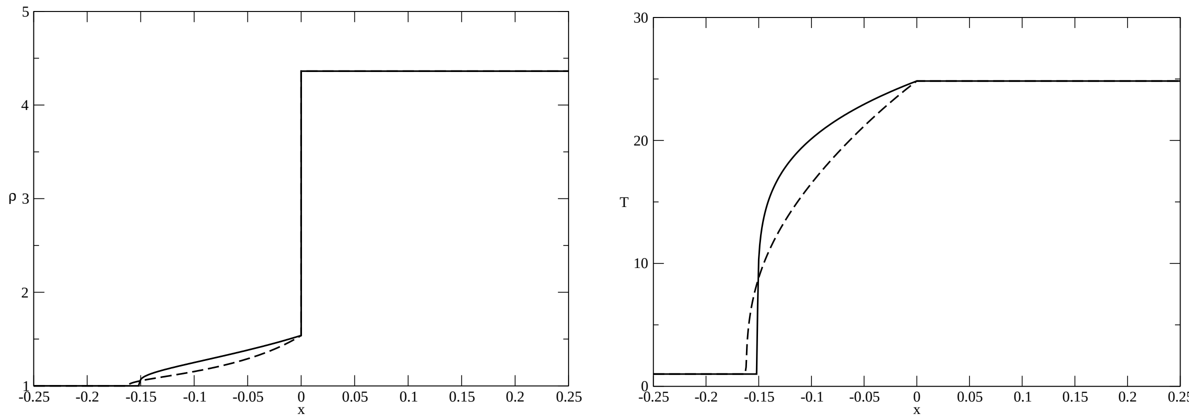

(a) Density (b) Temperature

Figure 6: Comparison of results from Fig. 3 (dashed line, $\kappa = 0.0001$) with results using $\kappa = (4\times 10^{-9})T^{7/2}/\rho$ (solid line). The coefficient of κ was chosen to give roughly the same precursor extent for each case.

[8] M. W. Sincell, M. Gehmeyr, and D. Mihalas, "The quasi-stationary structure of radiating shock waves. I. The one-temperature fluid.," *Shock Waves*, vol. 9, no. 6, pp. 391 – 402, 1999.

[9] M. W. Sincell, M. Gehmeyr, and D. Mihalas, "The quasi-stationary structure of radiating shock waves. II. The two-temperature fluid.," *Shock Waves*, vol. 9, no. 6, pp. 403 – 11, 1999.

[10] C. P. Wang, "Effect of thermal radiation on the propagation of plane shock waves.," *Physics of Fluids*, vol. 13, no. 7, pp. 1717 – 24, 1970.